

1

2

3

4 A LASSO-based reduced-form CMAQ model for predicting ozone and PM_{2.5}
5 responses to emission changes in South Korea

6

7

8 Da-Bin Lee¹, Hyun-Uk Kang¹, Gaeun Seo¹, Jinseok Kim^{2,3}, Bomi Kim^{3,4}, Jung-Hun Woo^{5,*}, and Kyu-
9 Baek Hwang^{1,*}

10

11

12

13 ¹Department of Computer Science and Engineering, Graduate School, Soongsil University, Seoul,
14 Republic of Korea

15 ²Environmental Planning Institute, Seoul National University, Seoul, Republic of Korea

16 ³Department of Advanced Technology Fusion, Konkuk University, Seoul, Republic of Korea

17 ⁴Department of Technology Fusion Engineering, Konkuk University, Seoul, Republic of Korea

18 ⁵Graduate School of Environmental Studies, Seoul National University, Seoul, Republic of Korea

19

20

21 *Corresponding authors

22 E-mail: woojh21@snu.ac.kr (J-HW), kbhwang@ssu.ac.kr (K-BH)

23 **Abstract**

24 Reduced-form models of the Community Multiscale Air Quality Modeling System (CMAQ) enable
25 efficient prediction of air quality responses to emission changes. In this study, we developed a reduced-
26 form CMAQ model based on the least absolute shrinkage and selection operator (LASSO) to
27 approximate CMAQ outputs in high-dimensional settings where the number of emission variables
28 exceeds the number of training samples. CMAQ simulations were generated using 118 emission
29 scenarios covering seven emission sectors across 17 provincial-level administrative regions in South
30 Korea. To account for the bounded nature of pollutant concentrations and to better represent nonlinear
31 responses, an adaptive logit transformation was applied within the LASSO framework. The model was
32 trained on 100 simulations and evaluated on 18 test scenarios, achieving mean root mean square errors
33 of 0.1 ppb for ozone and 0.1 $\mu\text{g}/\text{m}^3$ for $\text{PM}_{2.5}$. The model also identifies a small subset of influential
34 sector–region emission variables, enabling interpretable analysis of emission impacts and supporting
35 the design of targeted emission scenarios. A web-based interface was developed to demonstrate the
36 applicability of the approach, allowing interactive exploration of pollutant responses to emission
37 changes. The reduced-form model enables rapid prediction of air quality responses with substantially
38 lower computational cost than CMAQ simulations.

39 **Introduction**

40 Air pollution poses significant risks to human health. Major pollutants, such as ozone and $PM_{2.5}$, are
41 associated with premature mortality, particularly from cardiovascular and respiratory diseases [1-5].
42 Controlling their ambient concentrations is therefore important and requires the regulation of precursor
43 emissions. However, predicting the effects of emission controls is challenging because of diverse
44 meteorological conditions and complex chemical reactions. Chemical transport models [6] are
45 extensively used for this purpose. Among them, the Community Multiscale Air Quality Modeling
46 System (CMAQ) is one of the most widely applied models [7].

47 CMAQ integrates meteorological and emissions data to simulate hourly pollutant concentrations but
48 requires substantial computational resources. For example, a single control-policy simulation over
49 several months can take multiple days on a typical computing server. As a result, comparing a large
50 number of emission control scenarios using CMAQ alone is impractical.

51 To address this issue, reduced-form models have been developed to approximate CMAQ responses to
52 emission changes. Among them, response surface models based on multidimensional kriging have been
53 proposed as fast surrogates for CMAQ [8, 9], and later improved by integrating principal components
54 analysis with statistical kriging for ozone prediction [10]. Polynomial-based response surface models
55 have also been developed [11]. Subsequent studies extended this framework using deep learning and
56 regression-based input selection methods [12, 13]. More recently, various deep learning approaches
57 have been explored for efficient emulation of CMAQ [14-17]. These approaches aim to efficiently
58 approximate CMAQ responses to emission changes using statistical or machine learning models.

59 However, air quality policy analysis often requires evaluating emission controls across multiple sectors
60 and regions, which can lead to a large number of emission variables. Because CMAQ simulations are
61 computationally expensive, the number of available training scenarios is typically limited. As a result,
62 the number of input variables may exceed the number of training samples, leading to a high-dimensional
63 regression setting that poses challenges for reliable model estimation. Many existing reduced-form

64 approaches have been developed for problems with relatively small numbers of emission variables.
65 Deep learning approaches have also been explored for CMAQ emulation, but they usually require large
66 training datasets and may be less suitable when the number of variables is large relative to the number
67 of training samples.

68 To address this challenge, we develop a reduced-form CMAQ model for efficiently evaluating emission
69 scenarios for ozone and PM_{2.5}. The emission inventory considered in this study includes 119 sector–
70 region emission variables, representing seven emission sectors across 17 provincial-level administrative
71 regions in South Korea. The proposed model is based on the least absolute shrinkage and selection
72 operator (LASSO) [18], a linear regression method that is well suited for problems with many predictors
73 and limited training data [19]. In addition to improving model generalization, LASSO performs variable
74 selection, allowing the identification of sector–region emission variables that most strongly influence
75 ozone and PM_{2.5} concentrations. Because ozone and PM_{2.5} concentrations often exhibit nonlinear
76 relationships with precursor emissions [20-23], we introduce a nonlinear transformation of the response
77 variable within the LASSO framework. The resulting model enables rapid prediction of hourly pollutant
78 concentrations while maintaining the ability to approximate CMAQ outputs. Consequently, the
79 proposed reduced-form model facilitates efficient evaluation of air quality responses to emission
80 changes.

81

82 **Materials and methods**

83 **CMAQ simulations**

84 The CMAQ simulation domain covered South Korea with 67×82 grid cells at a spatial resolution of 9
85 km \times 9 km. Baseline emissions were based on the 2015 national emission inventory provided by the
86 National Institute of Environmental Research, Korea, through an official data request in July 2018. The
87 original emission source categories were aggregated into seven sectors: Power, Industry, Residential,

88 Solvent, Mobile, Agriculture, and Others (S1 Table). Emissions were reported for the 17 provincial-
89 level administrative regions in South Korea (hereafter regions; Fig 1).

90

91 **Fig 1. CMAQ simulation domain.** The 17 provincial-level administrative regions are shown in
92 different colors, with their names indicated.

93

94 Emission control scenarios were generated by randomly scaling each of the 119 sector-region emission
95 variables (7 sectors \times 17 regions) between 0.5 (50% reduction) and 1.5 (50% increase). Using Latin
96 hypercube sampling [24], 118 scenarios were generated to evenly cover this range. Emissions for these
97 scenarios were converted to hourly values for all grid cells using the SMOKE-Asia model [25] and used
98 as inputs to CMAQ.

99 Meteorological inputs were generated from the Weather Research and Forecasting model version 3.9.1
100 [26] with 2017 as the reference year. CMAQ version 4.7.1 [27] was run for four representative
101 months—January, April, July, and October—representing winter, spring, summer, and fall. These
102 simulations produced hourly ozone and PM_{2.5} concentrations for all grid cells over 123 days (31 days
103 for January, July, and October; 30 days for April). Hourly concentrations were extracted for each grid
104 cell and used to train and evaluate the reduced-form models.

105

106 **Machine learning-based reduced-form CMAQ models**

107 A reduced-form CMAQ model was developed to learn the relationship between emission control
108 scenarios and pollutant concentrations using the CMAQ simulations described above. Each scenario
109 was represented by 119 input variables corresponding to emission scaling factors for seven sectors
110 across 17 regions.

111 Among the 118 CMAQ simulations, 100 were used for training and 18 for evaluation. Each example
112 consisted of an emission control scenario and the corresponding CMAQ-simulated ozone or PM_{2.5}

113 concentrations. The number of predictors (119) exceeds the number of training samples (100), resulting
114 in a high-dimensional regression setting.

115 The model predicts hourly pollutant concentrations for each grid cell and time step. Separate models
116 were built for ozone and PM_{2.5}, and independent models were trained for each grid cell and hour. In
117 total, 16,218,288 models (24 hours × 123 days × 5,494 grid cells) were trained for each pollutant, each
118 mapping the 119 emission variables to a single concentration value at a specific grid cell and hour.

119 The reduced-form model is based on LASSO, which performs coefficient shrinkage and variable
120 selection. The regularization parameter λ was selected using five-fold cross-validation on the training
121 data. In some cases, the training responses showed little variation across emission scenarios. When the
122 number of unique response values in the training data was five or fewer, LASSO training was skipped
123 and the mean response value was used instead.

124 Because ozone and PM_{2.5} concentrations are nonnegative and exhibit nonlinear relationships with
125 precursor emissions, we applied an adaptive logit transformation to the response variable:

$$126 \quad \log\left(\frac{Y}{y_{upper}-Y}\right), \quad (1)$$

127 where Y is the pollutant concentration and y_{upper} is defined as the maximum concentration in the training
128 data plus its standard deviation. This transformation constrains predictions within the range $(0, y_{upper})$
129 and improves the ability of the linear model to represent nonlinear concentration responses.

130 Model performance was evaluated using the root mean square error (RMSE) between predicted and
131 CMAQ-simulated concentrations. To ensure robust evaluation, the 118 scenarios were randomly
132 divided into training and test sets (100 and 18 scenarios), and this procedure was repeated ten times
133 with different random splits. RMSE values were averaged across the repetitions.

134

135 **Results**

136 **Prediction accuracy of the reduced-form model**

137 This subsection evaluates the prediction accuracy of the proposed reduced-form CMAQ model. Using
138 100 CMAQ simulations for training, the reduced-form model reproduced CMAQ outputs with high
139 accuracy. In the CMAQ simulations, the average ozone concentration was 41.5 ppb. The reduced-form
140 model achieved a mean RMSE of approximately 0.1 ppb across all grid cells and hourly predictions,
141 indicating that the prediction error is small relative to the magnitude of the simulated concentrations.
142 Similarly, the average PM_{2.5} concentration in the CMAQ simulations was 12.1 µg/m³. The reduced-
143 form model produced a mean RMSE of approximately 0.1 µg/m³, again indicating high predictive
144 accuracy.

145 Figure 2 compares the CMAQ-simulated concentrations to the reduced-form model predictions for the
146 test scenarios. The predictions closely follow the one-to-one line for both ozone ($R^2 = 0.9998$) and PM_{2.5}
147 ($R^2 = 0.9997$), indicating that the reduced-form model accurately reproduces CMAQ variability across
148 grid cells and time steps.

149

150 **Fig 2. Scatterplots comparing CMAQ-simulated and model-predicted pollutant concentrations.**

151 Each point represents a grid cell-hour pair from the test scenarios for (A) ozone and (B) PM_{2.5}. Due to
152 the large number of comparisons (18 test scenarios × 10 trials × 16,218,288 grid cell-hour pairs), 25%
153 of the total data points are shown, while the reported R^2 and RMSE values are computed using the full
154 dataset.

155

156 In some grid cells, particularly outside the 17 regions (e.g., ocean cells), the training data showed little
157 variation across emission scenarios, so LASSO models were not fitted for those cells. As described in
158 Materials and methods, the mean response value was used in such cases. Although this occurred in
159 about 10% of all grid cells for ozone, it was uncommon within the 17 regions that are the focus of the
160 analysis (S2 Table).

161

162 **Spatial distribution of prediction errors**

163 To examine spatial variations in model accuracy, RMSE values were calculated separately for each grid
164 cell by aggregating prediction errors across all test scenarios and hourly predictions. Figure 3 shows the
165 spatial distribution of RMSE for ozone and PM_{2.5} concentrations. Overall, prediction errors remained
166 small across most regions of South Korea. For ozone, RMSE values were typically around 0.1 ppb, with
167 somewhat higher errors (up to about 0.5 ppb) observed in several localized areas. For PM_{2.5}, RMSE
168 values were also generally close to 0.1 µg/m³. Slightly higher errors (around 0.5 µg/m³) were observed
169 in a small number of localized areas (roughly two), and a single localized area showed higher errors
170 reaching approximately 0.8 µg/m³.

171

172 **Fig 3. Spatial distribution of prediction errors.** RMSE values for each grid cell for (A) ozone and
173 (B) PM_{2.5}.

174

175 S1 Fig shows the spatial distribution of the standard deviation of CMAQ-simulated pollutant
176 concentrations, which is similar to the pattern in Fig 3. This suggests that errors were higher in areas
177 with greater concentration variability.

178

179 **Interpretation of LASSO coefficients**

180 A key advantage of LASSO is its interpretability. Each coefficient in an individual LASSO model
181 represents the influence of emissions from a specific sector in a specific region on ozone or PM_{2.5}
182 concentrations at a particular location (grid cell) and time (hour). Across these models, an average of
183 23.5 variables for ozone and 22.0 for PM_{2.5} had nonzero coefficients, meaning that only about 20% of
184 the 119 emission variables were used to predict concentrations. This sparsity indicates that the model
185 effectively selected the most influential emission variables.

186

187 **Sectoral influence across regions**

188 To examine the overall influence of emission sectors, coefficients from LASSO models for grid cell-
189 hour pairs within the 17 regions were aggregated. For each sector, the absolute values of coefficients
190 associated with its sector–region emission variables were summed across all models. The influence
191 ratio for each sector was then calculated by dividing this sector-specific sum by the total sum across all
192 sectors. The direction of influence of a sector was determined from the signed sum of the coefficients
193 for that sector. These influence ratios and directions represent the overall effects of each sector across
194 the 17 regions, averaged over grid cells and time steps.

195 Figure 4A shows the sectoral influences on ozone responses. The Mobile sector dominated the ozone
196 response, accounting for 57.0% of the total influence. Most sectoral influences were negative, indicating
197 that increased emissions from many sectors were associated with lower ozone concentrations. In
198 contrast, emissions from the Solvent and Others sectors were generally associated with increased ozone
199 concentrations.

200

201 **Fig 4. Sectoral influences across the 17 regions.** Sectoral influence ratios for (A) ozone and (B) PM_{2.5}
202 are shown. The colors of the ratio values indicate the direction of influence (positive in green, negative
203 in red).

204

205 Figure 4B shows the sectoral influences on PM_{2.5} responses aggregated across the 17 regions. The
206 Agriculture sector had the largest influence (36.5%), followed by Industry (19.9%) and Mobile (18.5%).
207 Unlike ozone, all sectoral influences were positive, indicating that increased emissions from these
208 sectors were associated with higher PM_{2.5} concentrations.

209

210 **Sector-region influence for individual regions**

211 To identify the most influential emission variables for each region, sector–region emission variables
212 were analyzed separately by region. For each region, the absolute values of coefficients associated with
213 each sector–region variable were summed across all models for grid cell-hour pairs within that region.
214 The influence ratio for each variable was then calculated by dividing this sum by the total sum across
215 all sector–region variables. The direction of influence of each sector-region variable was determined
216 from the signed sum of its coefficients. The five variables with the largest influence ratios were
217 identified as the most influential variables for each region (S2 and S3 Figs).

218 Across regions, the combined influence ratios of the top five variables ranged from 50.2% to 78.0% for
219 ozone and 34.0% to 69.8% for PM_{2.5}, indicating that pollutant responses in each region were
220 substantially influenced by a limited number of emission variables.

221 For ozone, the Mobile sector was consistently among the most influential variables across all regions.
222 In many regions, ozone concentrations were influenced not only by local emissions but also by
223 emissions from nearby regions, reflecting regional transport.

224 For PM_{2.5}, influential variables varied more across regions. The most influential variables were mainly
225 from the Agriculture, Industry, Others, and Mobile sectors, although their relative importance differed
226 by region. As with ozone, emissions from nearby regions often appeared among the most influential
227 variables, indicating the importance of cross-regional effects.

228

229 **Emission scenario design and evaluation**

230 To demonstrate how the coefficient analysis can inform emission scenario design, we evaluated
231 example scenarios based on the sector–region variables identified in the previous subsection. Seoul was
232 selected for ozone and Jeju for PM_{2.5}, as the five most influential variables accounted for the largest
233 shares of total influence in these regions (78.0% and 69.8%, respectively; see S2C and S3Q Figs).
234 Emission scenarios were constructed by modifying these five variables for each selected region.

235 Starting from the baseline emissions, two scenarios were considered: a 10% reduction and a 10%
236 increase in emissions for the selected variables, while all other emissions were held constant. The
237 trained LASSO models were then used to predict the resulting changes in pollutant concentrations
238 across the simulation domain.

239 For ozone in Seoul, a 10% reduction in the five most influential variables increased the annual mean
240 concentration by 10.0% (12.0 to 13.2 ppb), whereas a 10% increase reduced it by 5.8% (12.0 to 11.3
241 ppb). For PM_{2.5} in Jeju, a 10% reduction decreased the annual mean concentration by 1.1% (9.3 to 9.2
242 µg/m³), while a 10% increase raised it by 1.1% (9.3 to 9.4 µg/m³).

243 These results demonstrate that the proposed approach can identify a small subset of influential emission
244 variables from a large candidate set and use them to construct targeted emission scenarios. In this study,
245 the LASSO models reduced the 119 sector–region variables to a small subset, enabling efficient
246 evaluation of emission control strategies focused on the most relevant sources.

247

248 **Web server for rapid emission scenario evaluation**

249 To facilitate practical use of the proposed model, we developed a web server that enables users to
250 evaluate emission scenarios interactively (<http://220.70.0.234:8080/>). Users can specify emission
251 changes for the sector–region emission variables, and the server then runs the LASSO-based reduced-
252 form CMAQ model to predict air quality responses.

253 The server displays the resulting annual mean ozone and PM_{2.5} concentrations on a map, showing grid
254 cell-level values along with the overall mean and range across all grid cells. When a user hovers over a
255 grid cell, the region containing the cell and the predicted annual mean concentration for that cell are
256 shown. When a cell is clicked, the server provides the five most influential sector–region variables for
257 that region along with their influence ratios. These variables provide guidance for designing targeted
258 emission scenarios for the selected region.

259 In addition to map-based visualization, the server allows users to download hourly concentration files
260 for the four simulated months (see Materials and methods). This enables more detailed analysis beyond
261 the annual mean summaries shown on the map.

262 The publicly available web server is deployed on a system equipped with an Intel(R) Core(TM) i7-7700
263 CPU at 4.20 GHz with 44 GB RAM, on which execution of the reduced-form models for both ozone
264 and PM_{2.5} requires less than 30 seconds. This demonstrates that the web server can provide rapid
265 evaluation of emission scenarios while retaining the spatial and temporal detail of CMAQ predictions.

266

267 **Discussion**

268 This study developed a LASSO-based reduced-form CMAQ model to efficiently evaluate air quality
269 responses to emission changes across multiple emission sectors and regions. The model achieved high
270 predictive accuracy for both ozone and PM_{2.5}, with very small RMSE values relative to the magnitude
271 of the concentrations and near-perfect agreement with CMAQ outputs. These results demonstrate that
272 the proposed approach can successfully approximate CMAQ responses despite the high-dimensional
273 input space and limited number of training scenarios. The adaptive logit transformation further
274 improved the model's ability to represent nonlinear concentration responses, which are commonly
275 observed for both ozone and PM_{2.5}.

276 A key advantage of the proposed approach is its ability to identify a small subset of influential emission
277 variables from a large set of sector-region combinations. Across all models, only about 20% of the 119
278 emission variables were selected, indicating substantial sparsity in the relationships between emissions
279 and pollutant concentrations. This sparsity enables meaningful interpretation of model coefficients and
280 facilitates the identification of key emission sources. The sectoral analysis showed that mobile
281 emissions dominated ozone responses, whereas agricultural emissions played the largest role in PM_{2.5}
282 formation. These findings are consistent with the known roles of NO_x emissions in ozone chemistry and

283 ammonia emissions in secondary $PM_{2.5}$ formation, supporting the physical plausibility of the model
284 results.

285 The results also highlight the importance of regional interactions in air quality responses. For both ozone
286 and $PM_{2.5}$, influential variables often included emissions from nearby regions, indicating that pollutant
287 concentrations are affected not only by local emissions but also by regional transport. This suggests that
288 effective air quality management requires coordinated emission control strategies across administrative
289 boundaries rather than region-specific policies alone.

290 The scenario analysis further demonstrates the utility of the proposed framework for emission scenario
291 evaluation. By focusing on a small number of influential variables, the model enables the design of
292 targeted emission scenarios that can produce meaningful changes in pollutant concentrations. For
293 example, in regions where the most influential variables explain a large fraction of the total influence,
294 such as Seoul for ozone and Jeju for $PM_{2.5}$, modifying these variables led to notable changes in
295 concentrations. Specifically, reducing emissions from the most influential variables in Seoul increased
296 ozone concentrations, whereas similar changes resulted in decreases in $PM_{2.5}$ concentrations in Jeju.
297 These contrasting responses between pollutants highlight the pollutant-specific nature of emission
298 impacts. Overall, the results illustrate how the model can provide insights into pollutant- and region-
299 specific responses and support the development of more effective and region-specific emission
300 scenarios.

301 Compared with existing reduced-form approaches, the proposed method is particularly well suited for
302 high-dimensional settings where the number of emission variables is large relative to the number of
303 training simulations. While deep learning models have been increasingly applied for CMAQ emulation,
304 they typically require large training datasets and may be less interpretable. In contrast, the LASSO-
305 based approach used here provides both computational efficiency and interpretability, making it suitable
306 for applications with limited training data and a need for transparent analysis of emission scenarios.

307 The developed web server was used to demonstrate the practical applicability of the proposed approach
308 by enabling rapid, interactive evaluation of emission scenarios. Through this interface, users can explore

309 air quality responses at the grid-cell level and identify key emission drivers for specific regions,
310 illustrating how the model can support intuitive and efficient scenario design. The ability to generate
311 predictions in under a minute highlights the computational efficiency of the reduced-form model
312 compared with traditional CMAQ simulations, which require substantially longer run times.
313 Despite the advantages of the proposed approach, several limitations should be noted. First, the model
314 was developed under fixed meteorological conditions based on a single reference year and does not
315 account for meteorological variability. However, because this study focuses on relative changes in
316 pollutant concentrations in response to emission perturbations, the use of a consistent reference year
317 provides a stable basis for comparison. Second, the model does not explicitly represent temporal
318 dynamics, as independent models were trained for each grid cell and time step. Third, emission
319 scenarios were constructed by independently scaling sector–region variables, whereas real-world
320 emission changes may involve dependencies across sectors and regions. Finally, the analysis is based
321 solely on CMAQ simulations and was not evaluated against observational data.
322 Future work could address these limitations by incorporating meteorological variability and temporal
323 dynamics into the modeling framework, enabling application beyond a single reference year. The
324 framework could also be extended to additional pollutants beyond ozone and PM_{2.5}.

325

326 **Conclusion**

327 This study developed a LASSO-based reduced-form CMAQ model to efficiently evaluate air quality
328 responses to emission changes across multiple sectors and regions. The model achieved high predictive
329 accuracy while substantially reducing computational cost compared with full CMAQ simulations. By
330 identifying a small subset of influential sector–region variables, the proposed approach enables efficient
331 interpretation of emission impacts and the design of targeted emission scenarios. Overall, the results
332 demonstrate that the proposed framework provides a practical and computationally efficient tool for
333 emission scenario evaluation with high-dimensional inputs.

334

335 **References**

- 336 1. Jerrett M, Burnett RT, Pope CA, 3rd, Ito K, Thurston G, Krewski D, et al. Long-term ozone
337 exposure and mortality. *N Engl J Med.* 2009;360(11):1085-95. doi: 10.1056/NEJMoa0803894. PubMed
338 PMID: 19279340; PubMed Central PMCID: PMCPMC4105969.
- 339 2. Pope CA, 3rd, Coleman N, Pond ZA, Burnett RT. Fine particulate air pollution and human
340 mortality: 25+ years of cohort studies. *Environ Res.* 2020;183:108924. Epub 20191114. doi:
341 10.1016/j.envres.2019.108924. PubMed PMID: 31831155.
- 342 3. de Bont J, Jaganathan S, Dahlquist M, Persson A, Stafoggia M, Ljungman P. Ambient air
343 pollution and cardiovascular diseases: An umbrella review of systematic reviews and meta-analyses. *J*
344 *Intern Med.* 2022;291(6):779-800. Epub 20220308. doi: 10.1111/joim.13467. PubMed PMID:
345 35138681; PubMed Central PMCID: PMCPMC9310863.
- 346 4. Dedoussi IC, Eastham SD, Monier E, Barrett SRH. Premature mortality related to United States
347 cross-state air pollution. *Nature.* 2020;578(7794):261-5. Epub 20200212. doi: 10.1038/s41586-020-
348 1983-8. PubMed PMID: 32051602.
- 349 5. Michelozzi P, Forastiere F, Fusco D, Perucci CA, Ostro B, Ancona C, et al. Air pollution and
350 daily mortality in Rome, Italy. *Occup Environ Med.* 1998;55(9):605-10. doi: 10.1136/oem.55.9.605.
351 PubMed PMID: 9861182; PubMed Central PMCID: PMCPMC1757645.
- 352 6. Gao Z, Zhou X. A review of the CAMx, CMAQ, WRF-Chem and NAQPMS models:
353 Application, evaluation and uncertainty factors. *Environ Pollut.* 2024;343:123183. Epub 20231216. doi:
354 10.1016/j.envpol.2023.123183. PubMed PMID: 38110047.
- 355 7. US EPA Office of Research and Development. CMAQ: Zenodo; 2024. Available from:
356 <https://doi.org/10.5281/zenodo.13883210>.
- 357 8. US EPA. Technical Support Document for the Proposed PM NAAQS Rule: Response Surface
358 Modeling. US Environmental Protection Agency Research Triangle Park, NC; 2006.
- 359 9. Foley KM, Napelenok SL, Jang C, Phillips S, Hubbell BJ, Fulcher CM. Two reduced form air
360 quality modeling techniques for rapidly calculating pollutant mitigation potential across many sources,
361 locations and precursor emission types. *Atmospheric Environment.* 2014;98:283-9. doi:
362 <https://doi.org/10.1016/j.atmosenv.2014.08.046>.
- 363 10. Porter PS, Rao ST, Hogrefe C, Mathur R. A Reduced Form Model for Ozone Based on Two
364 Decades of CMAQ Simulations for the Continental United States. *Atmos Pollut Res.* 2017;8(2):275-
365 84. doi: 10.1016/j.apr.2016.09.005. PubMed PMID: 30245573; PubMed Central PMCID:
366 PMCPMC6145467.

- 367 11. Xing J, Ding D, Wang S, Zhao B, Jang C, Wu W, et al. Quantification of the enhanced
368 effectiveness of NO_x control from simultaneous reductions of VOC and NH₃ for reducing air pollution
369 in the Beijing–Tianjin–Hebei region, China. *Atmos Chem Phys*. 2018;18(11):7799-814. doi:
370 10.5194/acp-18-7799-2018.
- 371 12. Li J, Dai Y, Zhu Y, Tang X, Wang S, Xing J, et al. Improvements of response surface modeling
372 with self-adaptive machine learning method for PM_{2.5} and O₃ predictions. *Journal of Environmental*
373 *Management*. 2022;303:114210. doi: <https://doi.org/10.1016/j.jenvman.2021.114210>.
- 374 13. Xing J, Zheng S, Ding D, Kelly JT, Wang S, Li S, et al. Deep Learning for Prediction of the
375 Air Quality Response to Emission Changes. *Environ Sci Technol*. 2020;54(14):8589-600. Epub
376 20200701. doi: 10.1021/acs.est.0c02923. PubMed PMID: 32551547; PubMed Central PMCID:
377 PMC7375937.
- 378 14. Payami M, Choi Y, Kayastha SG, Park J. Emulating CMAQ using deep learning: A
379 comparative study on simulating surface NO₂, O₃, and PM_{2.5} over the CONUS using the
380 EQUATES dataset. *Sci Total Environ*. 2025;1000:180467. Epub 20250916. doi:
381 10.1016/j.scitotenv.2025.180467. PubMed PMID: 40946609.
- 382 15. Lee Y, Park J, Kim J, Woo J-H, Lee J-H. Rapid PM_{2.5}-Induced Health Impact Assessment: A
383 Novel Approach Using Conditional U-Net CMAQ Surrogate Model. *Atmosphere*. 2024;15(10):1186.
384 PubMed PMID: doi:10.3390/atmos15101186.
- 385 16. Xing J, Zheng S, Li S, Huang L, Wang X, Kelly JT, et al. Mimicking atmospheric
386 photochemical modelling with a deep neural network. *Atmos Res*. 2022;265:1-11. doi:
387 10.1016/j.atmosres.2021.105919. PubMed PMID: 34857979; PubMed Central PMCID:
388 PMC8630640.
- 389 17. Lee Y, Park J, Kim J, Woo J-H, Lee J-H. Conditional UNet emulation of CMAQ simulations
390 for fine particulate matter concentration prediction. *Scientific Reports*. 2025;15(1):38616. doi:
391 10.1038/s41598-025-22388-2.
- 392 18. Tibshirani R. Regression Shrinkage and Selection via the Lasso. *Journal of the Royal Statistical*
393 *Society Series B (Methodological)*. 1996;58(1):267-88.
- 394 19. Tibshirani RJ. The lasso problem and uniqueness. *Electron J Statist*. 2013;7:1456-90. doi:
395 10.1214/13-EJS815.
- 396 20. Xing J, Wang SX, Jang C, Zhu Y, Hao JM. Nonlinear response of ozone to precursor emission
397 changes in China: a modeling study using response surface methodology. *Atmos Chem Phys*.
398 2011;11(10):5027-44. doi: 10.5194/acp-11-5027-2011.
- 399 21. Xiao X, Cohan DS, Byun DW, Ngan F. Highly nonlinear ozone formation in the Houston region
400 and implications for emission controls. *Journal of Geophysical Research: Atmospheres*. 2010;115(D23).

401 doi: <https://doi.org/10.1029/2010JD014435>.

402 22. Zhao N, Zhang H, Wang G. Revealing the nonlinear responses of PM_{2.5} and O₃ to VOC and
403 NO_x emissions from various sources in Shandong, China. *Journal of Hazardous Materials*.
404 2025;489:137655. doi: <https://doi.org/10.1016/j.jhazmat.2025.137655>.

405 23. Sillman S, He D. Some theoretical results concerning O₃-NO_x-VOC chemistry and NO_x-VOC
406 indicators. *J Geophys Res*. 2002;107(D22):4659. doi: 10.1029/2001JD001123.

407 24. McKay MD, Beckman RJ, Conover WJ. A Comparison of Three Methods for Selecting Values
408 of Input Variables in the Analysis of Output from a Computer Code. *Technometrics*. 1979;21(2):239-
409 45. doi: 10.2307/1268522.

410 25. Woo J-H, Choi K-C, Kim HK, Baek BH, Jang M, Eum J-H, et al. Development of an
411 anthropogenic emissions processing system for Asia using SMOKE. *Atmospheric Environment*.
412 2012;58:5-13. doi: <https://doi.org/10.1016/j.atmosenv.2011.10.042>.

413 26. Skamarock WC, Klemp JB, Dudhia J, Gill DO, Barker DM, Duda MG, et al. A Description of
414 the Advanced Research WRF Version 3. NCAR Technical Note NCAR/TN-475+STR June 2008
415 Mesoscale and Microscale Meteorology Division National Center for Atmospheric Research Boulder.
416 2008;475:1. doi: 10.5065/d68s4mvh.

417 27. US EPA Office of Research and Development. CMAQv4.7.1: Zenodo; 2010. 4.7.1:[Available
418 from: <https://doi.org/10.5281/zenodo.1079879>.

419

420

421 **Supporting information**

422 **S1 Fig. Spatial distribution of pollutant concentration variability.** Standard deviation of CMAQ-
423 simulated pollutant concentrations for each grid cell, for (A) ozone and (B) PM_{2.5}.

424 **S2 Fig. Influence ratios of the top five sector-region emission variables for ozone in individual**
425 **regions.** Regions: (A) Incheon, (B) Gyeonggi, (C) Seoul, (D) Gangwon, (E) Chungbuk, (F) Sejong, (G)
426 Daejeon, (H) Chungnam, (I) Gyeongbuk, (J) Daegu, (K) Ulsan, (L) Busan, (M) Gyeongnam, (N)
427 Jeonbuk, (O) Gwangju, (P) Jeonnam, and (Q) Jeju. The colors of the ratio values indicate the direction
428 of influence (positive in green, negative in red). The value in the lower right corner of each plot indicates
429 the sum of the top five influence ratios.

430 **S3 Fig. Influence ratios of the top five sector-region emission variables for PM_{2.5} in individual**
431 **regions.** Regions: (A) Incheon, (B) Gyeonggi, (C) Seoul, (D) Gangwon, (E) Chungbuk, (F) Sejong, (G)
432 Daejeon, (H) Chungnam, (I) Gyeongbuk, (J) Daegu, (K) Ulsan, (L) Busan, (M) Gyeongnam, (N)
433 Jeonbuk, (O) Gwangju, (P) Jeonnam, and (Q) Jeju. The colors of the ratio values indicate the direction
434 of influence (positive in green, negative in red). The value in the lower right corner of each plot indicates
435 the sum of the top five influence ratios.

436 **S1 Table. Grouping of the emission source categories into seven sectors.**

437 **S2 Table. Cases with insufficient variation for model training.** A total of 162,182,880 cases were
438 considered (5,494 cells × 123 days × 24 hours × 10 trials), of which 46,936,800 correspond to the 17
439 regions (1,590 cells × 123 days × 24 hours × 10 trials).

This manuscript is a preprint and has not been peer reviewed. The copyright holder has made the manuscript available under a Creative Commons Attribution 4.0 International (CC BY) [license](https://creativecommons.org/licenses/by/4.0/) and consented to have it forwarded to [EarthArXiv](https://eartharxiv.org/) for public posting.

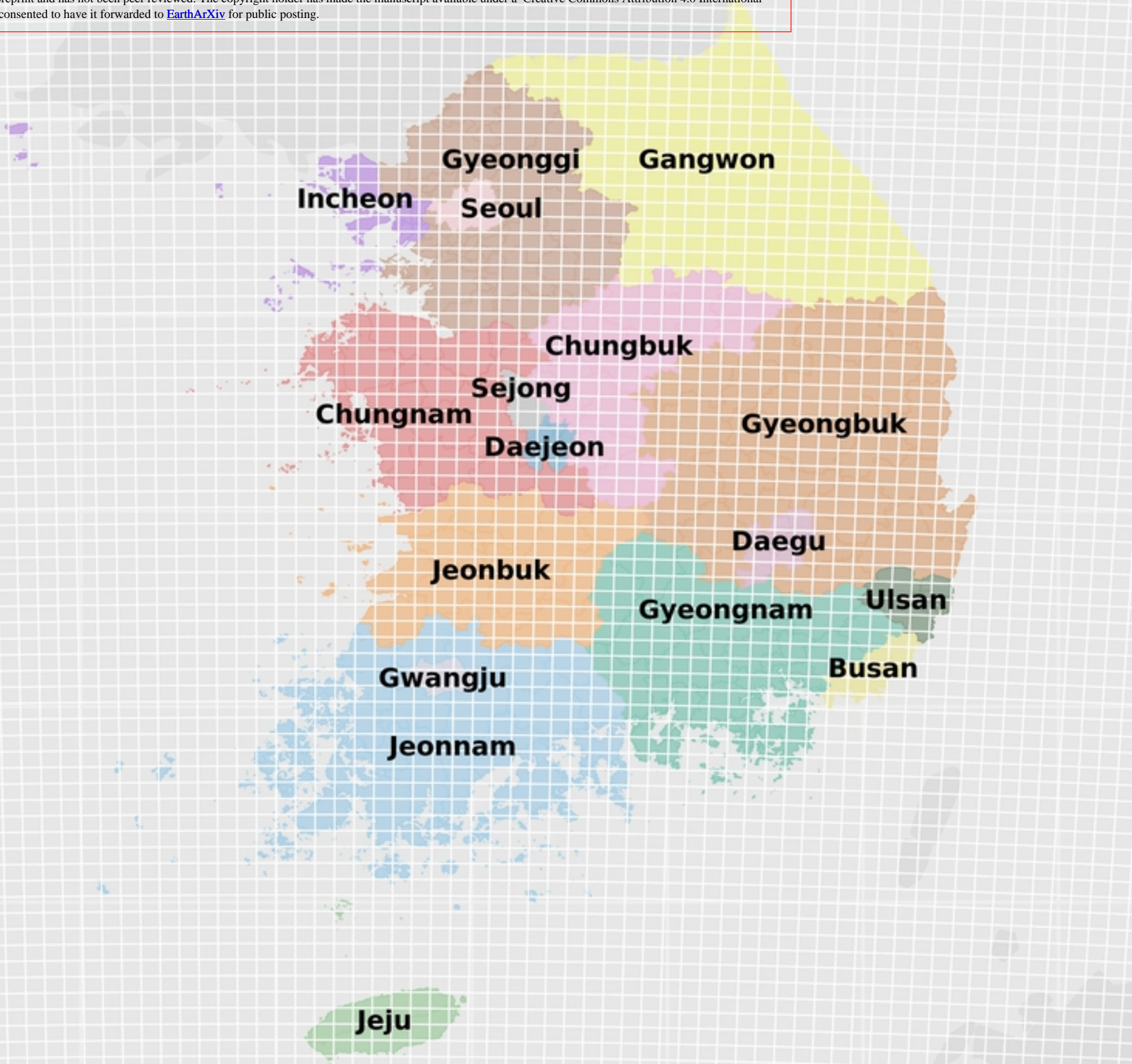


Fig 1

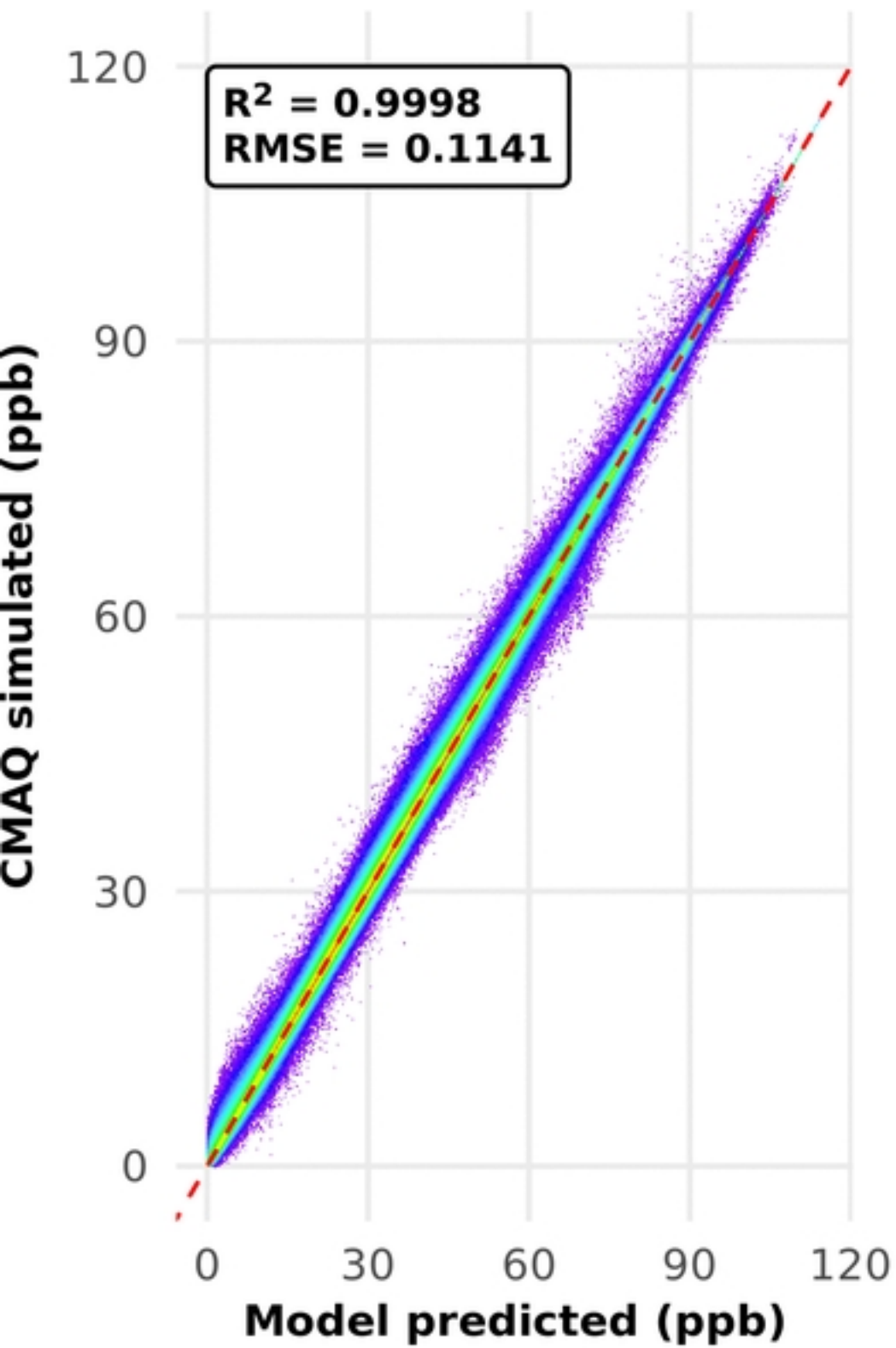
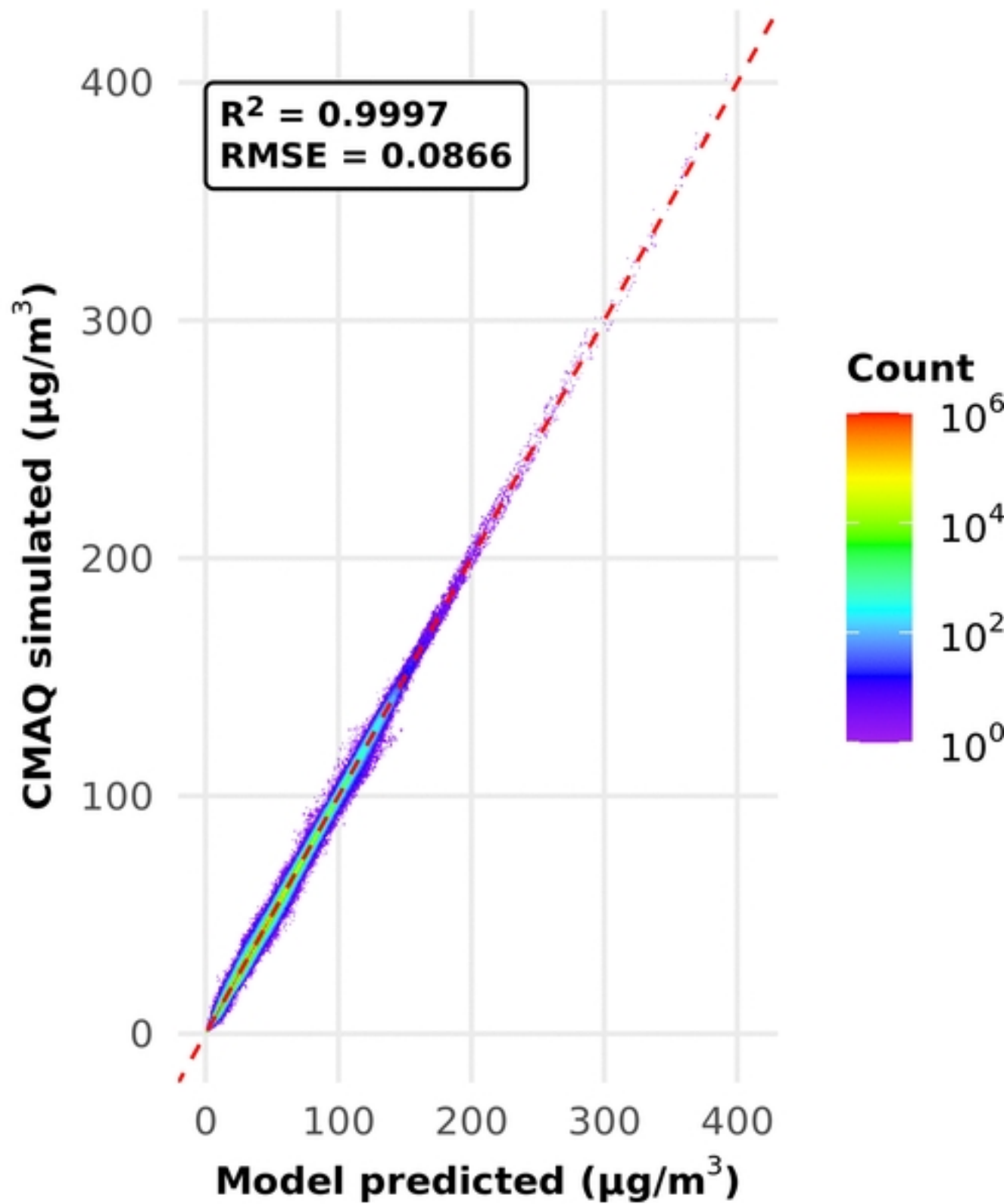
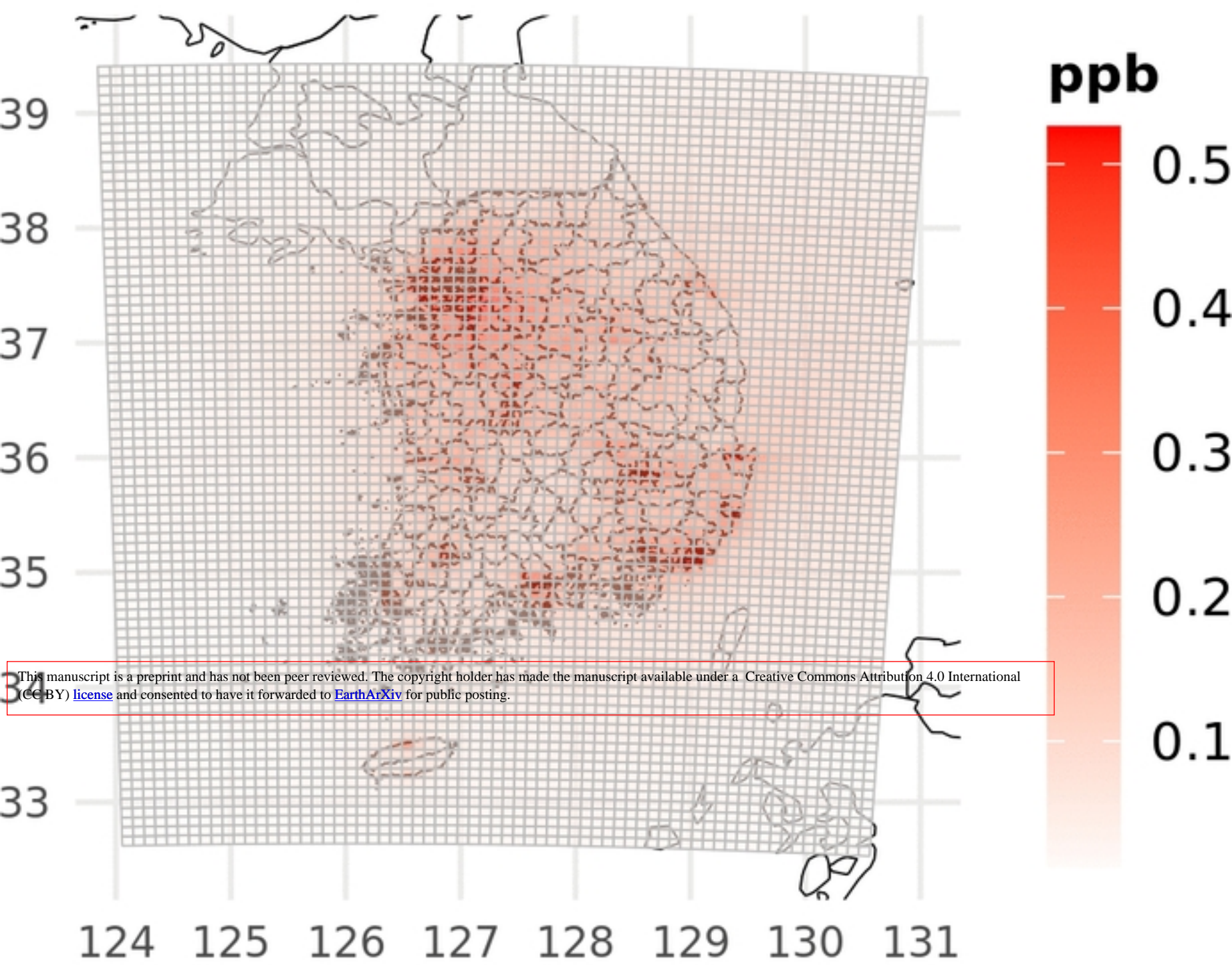
(A) Ozone**(B) PM_{2.5}**

Fig 2

(A) Ozone



(B) PM_{2.5}

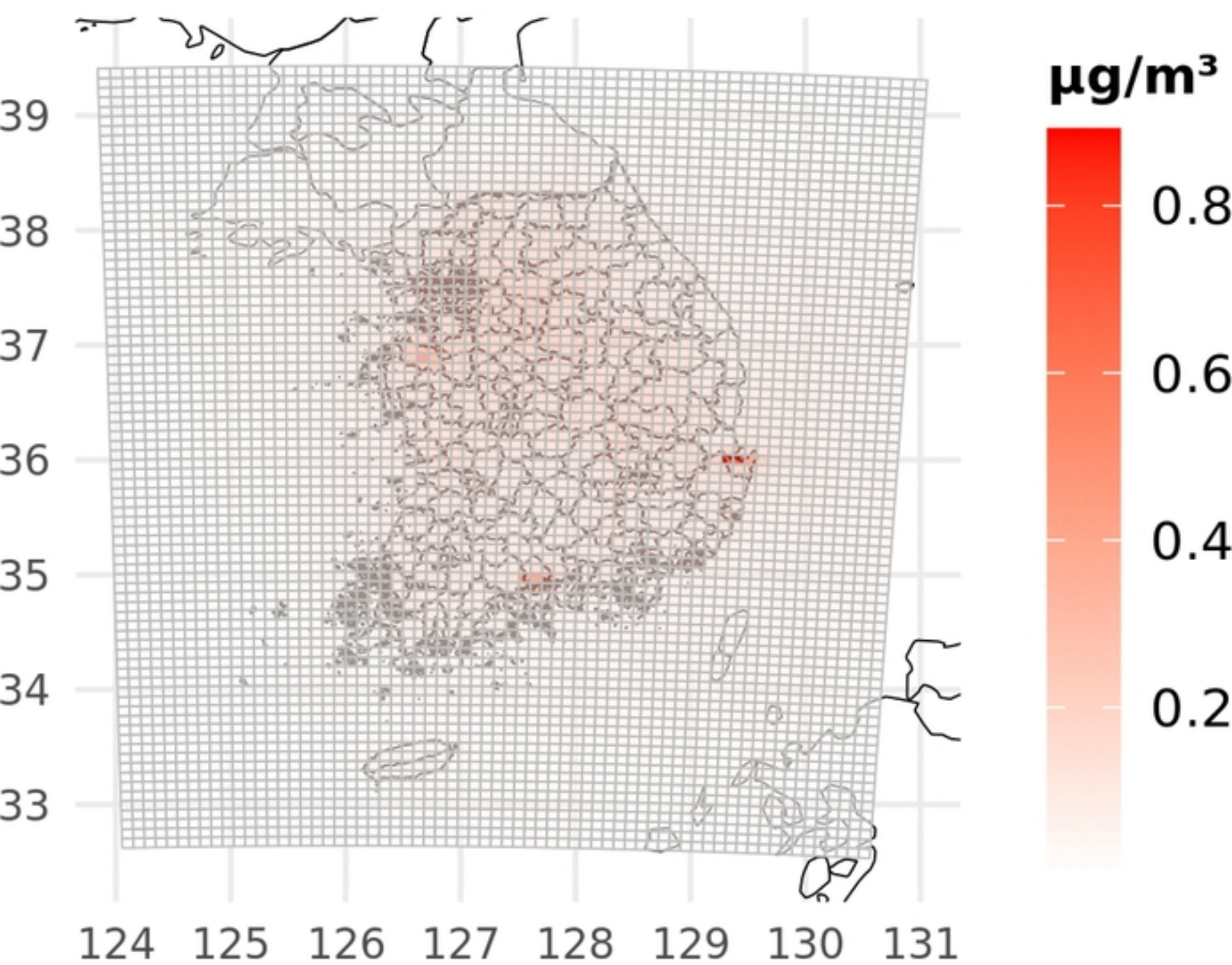


Fig 3

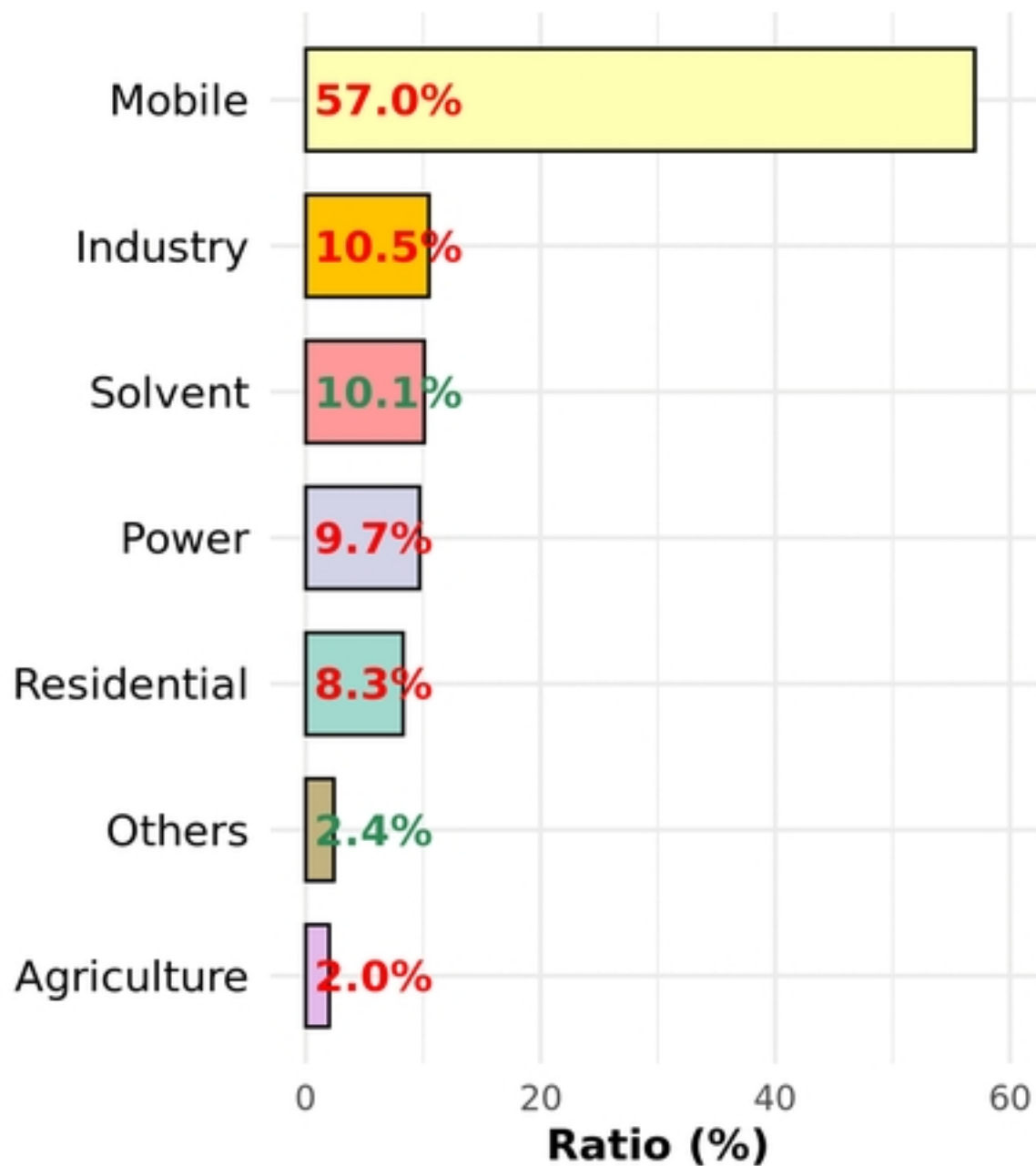
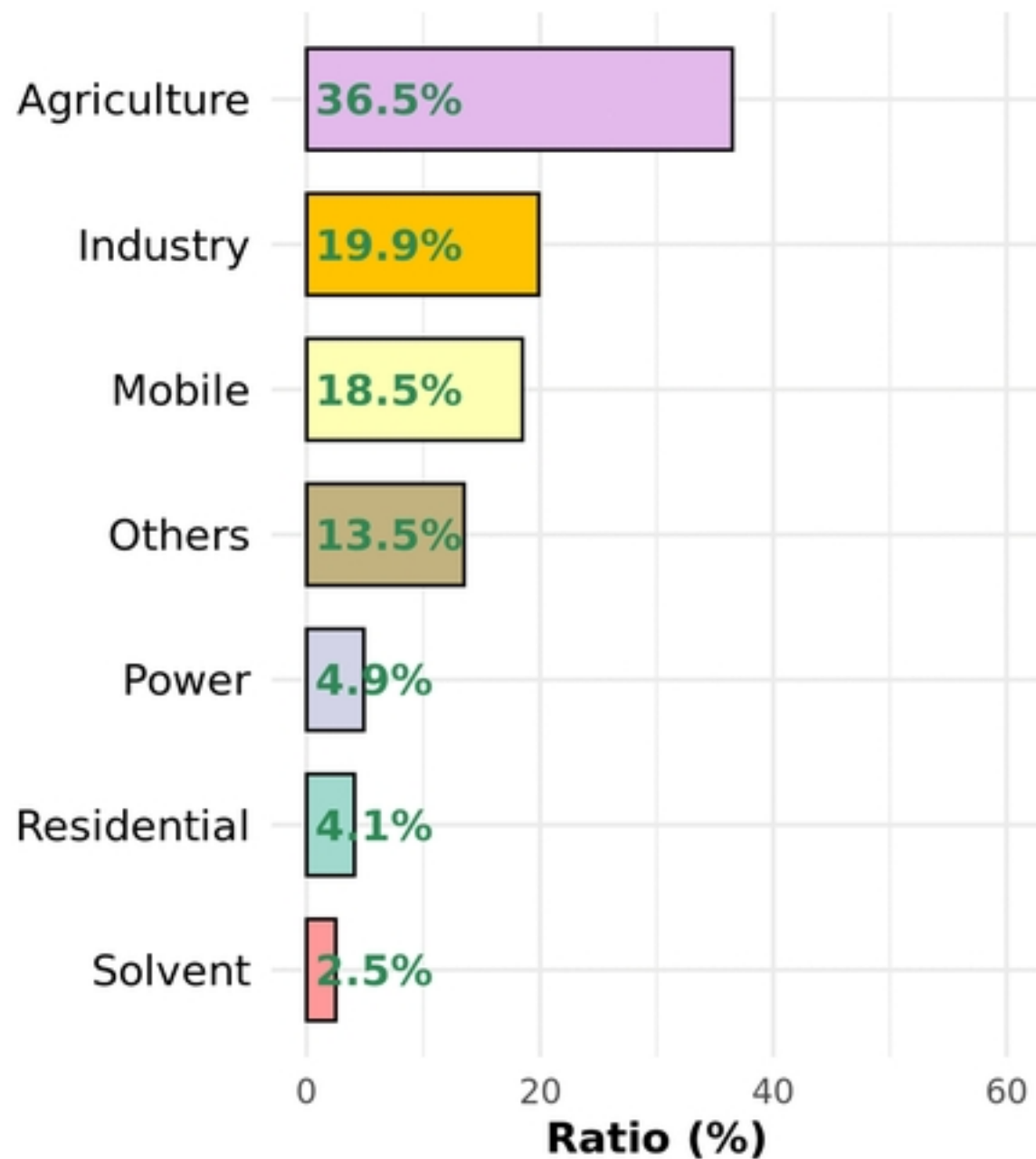
(A) Ozone**(B) PM_{2.5}**

Fig 4